An experimental study of starting plumes over area sources (*)(**)

M. J. FRIEDL, C. HÄRTEL and T. K. FANNELØP
Institute of Fluid Dynamics, Swiss Federal Institute of Technology
CH-8092 Zürich, Switzerland

(ricevuto il 18 Novembre 1998; approvato il 6 Maggio 1999)

Summary. — Experiments have been performed to study the dynamics of plumes which develop, if buoyant fluid enters a homogeneous, unstratified environment through a source of finite width. The experiments were conducted in a cubic tank of salt water with 0.8m side length into which dyed fresh water was released at a constant volume-flow rate through a circular felt at the bottom. The governing non-dimensional parameter of the flow, namely the ratio of inflow velocity to buoyancy velocity, was varied over more than two orders of magnitude in the experiments. The flow is shown to pass through two distinct phases, and a new integral model is presented which describes the flow in the early stage. For later times and at larger distances from the source, the flow is found to be well described by Turner's model for starting plumes from point sources.

PACS 92.10.Lq – Turbulence and diffusion.
PACS 47.20.Bp – Buoyancy-driven instability.
PACS 47.55.Hd – Stratified flows.
PACS 01.30.Cc – Conference proceedings.

1. – Introduction

Plumes are encountered in many geophysical situations, examples being hot magma rising in the Earth's mantle [1], water, heated by volcanic activities on the sea bed, rising in the ocean [2], or ascending masses of warm air that lead to the formation of clouds in the atmosphere. In industrial safety and environmental protection, the study of plumes is also of substantial interest, because they may result from the accidental release of—possibly hazardous—gases or vapors lighter than air [3]. An example is the

(*) Paper presented at the International Workshop on "Vortex Dynamics in Geophysical Flows", Castro Marina (LE), Italy, 22-26 June 1998.
(**) The authors of this paper have agreed to not receive the proofs for correction.

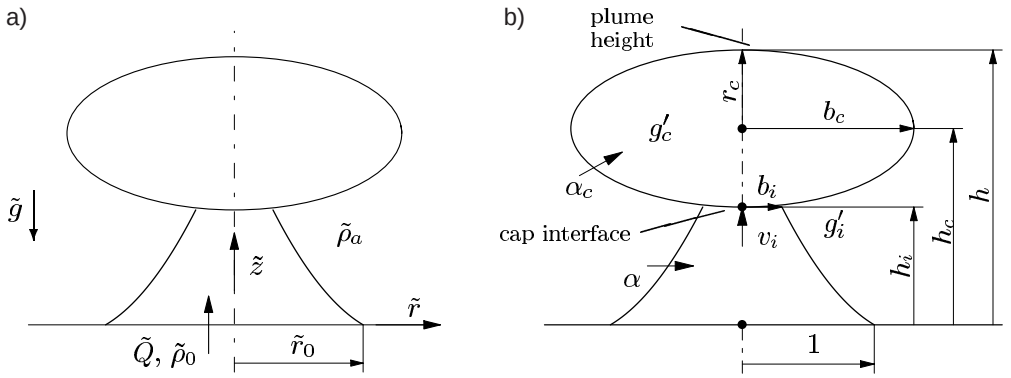

Fig. 1. – Sketch of a starting plume above an area source. a) Starting at time $\tilde{t} = 0$, a constant volume flux $\tilde{Q}$ of fluid with density $\tilde{\varrho}_0$ is released through a circular area source with radius $\tilde{r}_0$ into an environment at rest (ambient density $\tilde{\varrho}_a > \tilde{\varrho}_0$). b) Related variables.

uncontrolled blow-out of natural gas from off-shore reservoirs that poses a substantial threat for ships and drilling installations. The natural gas that forms a bubble plume within the water, is eventually set free into the atmosphere where it rises further due to its smaller density [4]. In this case a safe assessment of the risk associated with explosive mixtures of gas and air requires a realistic prediction of the flow especially close to the so-called boiling area on the sea surface where the natural gas is released into the atmosphere.

So far, most studies on plumes have considered the flow at distances from its origin large enough to assure that the flow structure is independent of conditions at the source or in the region of formation. Based on this assumption, integral models have been developed for steady plumes [5] and starting plumes [6]. A detailed account of the classical theories in this field can be found in [3, 7]. In the present paper we will focus on the early flow development of plumes which originate from area sources of finite width where buoyant fluid is released at a constant-volume flow rate. A sketch of the basic situation is provided in fig. 1a, where $\tilde{r}$ and $\tilde{z}$ are the radial and axial directions, respectively (a tilde denotes a dimensional quantity here). At time $\tilde{t} = 0$, buoyant fluid with density $\tilde{\varrho}_0$ is released into an environment of density $\tilde{\varrho}_a > \tilde{\varrho}_0$ from a circular area source with radius $\tilde{r}_0$, located in the bottom boundary of the reservoir.

An idea of the developing unsteady flow above the source can be gained from fig. 2, where photographs are shown from one of our experiments which are described in more detail in sect. 3. In our experiments the plume is formed of dyed fresh water which rises in an environment of salt water. During the start-up phase of the flow the development of an intense vortex ring can be observed (see fig. 2b) which we will refer to herein as the initial cap. This initial cap rises followed by a slender plume which accelerates and gets narrower with increasing distance from the source (fig. 2c, d). At a certain height, the plume is then observed to break through the initial cap and to rise further topped by a new cap (fig. 2e). It will become evident from the results presented below that the breakthrough of the plume marks the transition from a starting flow which is largely determined by the source conditions, to a fully developed state. For larger heights $\tilde{z}$ the latter is well described by the classical theory of starting plumes from point sources [6].

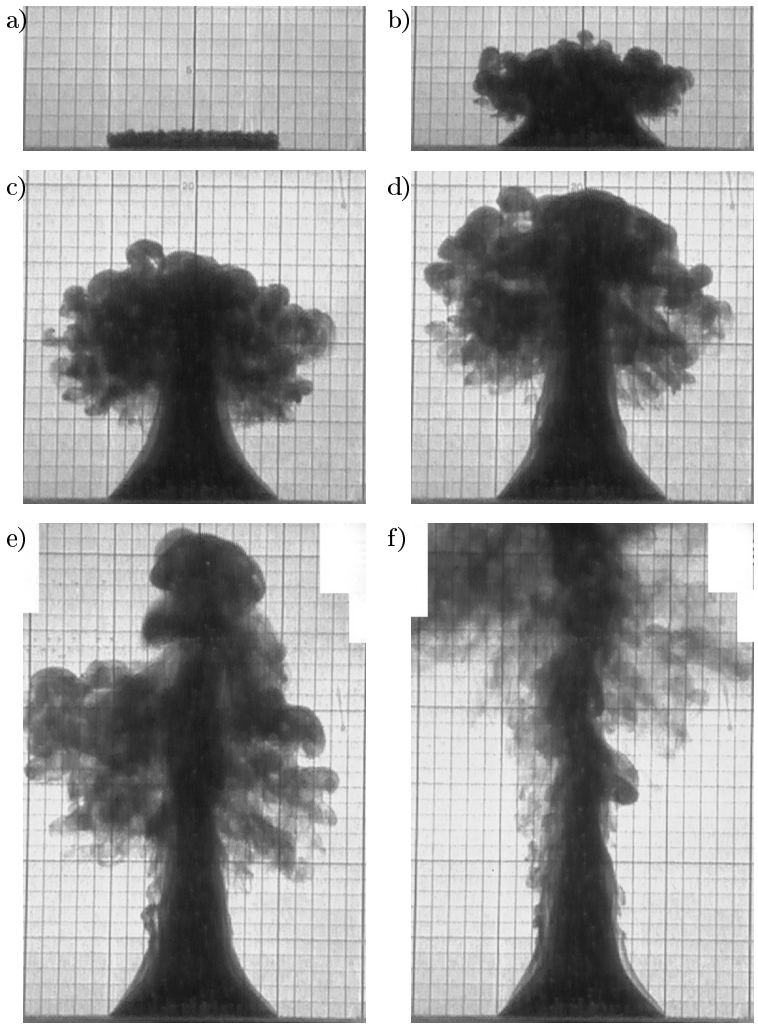

Fig. 2. – Evolution of a starting plume from an area source for $F = 0.125$ (see eq. (2)). The spacing of the background mesh is 1 cm. Pictures taken at non-dimensional times t of 2.14 (a), 4.05 (b), 7.05 (c), 8.27 ($= t^*$) (d), 10.14 (e), 16.72 (f).

2. – Governing parameters

To achieve a non-dimensional description of the problem, we choose the radius $\tilde{r}_0$ of the area source (see fig. 1a) and the reduced gravitational acceleration $\tilde{g}'_0 = \tilde{g}(\tilde{\varrho}_a - \tilde{\varrho}_0)/\tilde{\varrho}_0$ as characteristic quantities. This leads to the following non-dimensional form of the spatial coordinates r, z and time t:

$$r = \tilde{r}/\tilde{r}_0, \qquad z = \tilde{z}/\tilde{r}_0, \qquad t = \tilde{t}\sqrt{\tilde{g}'_0/\tilde{r}_0}\,. \tag{1}$$

If we consider the Boussinesq limit of small density differences where $\tilde{\varrho}_0 \approx \tilde{\varrho}_a$, the flow

is governed by the following three-dimensionless parameters [8]

$$(2) \qquad \nu = \frac{\tilde{\nu}}{\tilde{r}_0 \sqrt{\tilde{r}_0 \tilde{g}(\tilde{\varrho}_a - \tilde{\varrho}_0)/\tilde{\varrho}_a}}, \qquad D = \frac{\nu}{\mathrm{Sc}}, \qquad F = \frac{\tilde{Q}}{\pi \tilde{r}_0^2 \sqrt{\tilde{r}_0 \tilde{g}(\tilde{\varrho}_a - \tilde{\varrho}_0)/\tilde{\varrho}_a}}.$$

Here ν denotes the kinematic viscosity, D the coefficient of molecular diffusion in the density field, and Sc the common Schmidt number which is a fluid property. Since our experiments were conducted with salt water and fresh water, the influence of diffusion on the density field is certainly negligible owing to the very high Schmidt number of salt in water ($\mathrm{Sc} = 770$). In (2) F is the dimensionless inflow velocity which represents the buoyancy flux per unit area at the source. We will denote this quantity as the buoyancy parameter here [3]. For steady plumes it is known that the buoyancy flux per unit area is the major parameter governing the flow [7].

3. – Experimental set-up

The experiments were performed in a cubic tank with transparent walls of 0.8 m side length. A sketch of the experimental set-up is given in fig. 3. The tank was filled with tap water in which cooking salt was dissolved to increase the density. The settling chamber below the tank and the cylinder shown on the right-hand side in fig. 3 were filled with fresh water, dyed with methylene blue. The settling chamber and the salt water tank were connected by a circular opening in which a 2 mm thick felt was mounted. This circular opening represents the area source, and the resistance of the felt was sufficient to keep the light fluid well separated from the brine before the experiment was started. By pushing the piston into the cylinder at a low but constant speed, a constant flux of fresh water was generated which entered the salt water reservoir through the area source. The piston was driven by a step motor which allowed

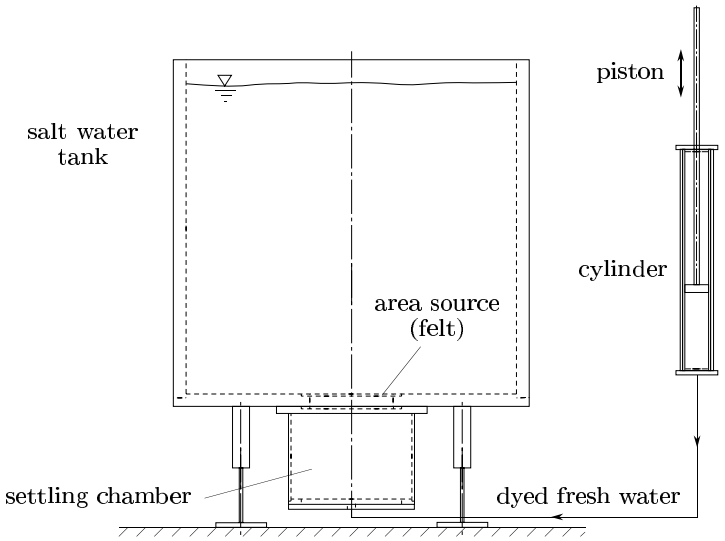

Fig. 3. – Sketch of the experimental set-up. The side length of the salt water tank is 0.8 m.

the volume flow rate $\tilde{Q}$ to be controlled with an accuracy of 0.1%. In our experiments $\tilde{Q}$ was typically of the order of 10^{-5} m^3/s.

The densities of brine and fresh water were determined by measuring the buoyancy force acting on a displacement body of known volume, when immersed in the fluid. This buoyancy force was measured with the aid of a high-precision balance and could be determined with an accuracy of 0.1%. During the experiments the flow development was registered by means of two video cameras. The rise of the plume of dyed fresh water was recorded against a light background consisting of an illuminated white sheet with a mesh of 1 cm spacing (see fig. 2). One camera focused on the region close to the source, the other recorded the plume in the upper half of the tank. From the video recordings, we determined several quantities as a function of time $\tilde{t}$, among these the actual height of the plume $\tilde{h}$ and the width $\tilde{b}_c$ of the initial cap.

4. – Phenomenology of the flow

In the phase immediately after the start of the experiment (see fig. 2a) the density interface between light and heavy fluid features a pronounced Rayleigh-Taylor–like instability which results in the development of small mushroom-shaped structures. These structures are very similar to structures that have been observed above other kinds of distributed sources of buoyancy such as heated surfaces [7, 9]. The significance of the interfacial instability to the further flow evolution is that eventually it leads to a thick layer of mixed fluid which lifts off the area source in the form of a buoyant vortex ring which is clearly seen in fig. 2b. The diameter of this vortex ring is set by the width of the area source and it is continuously fed with light fluid which rises within the slender plume. From fig. 2b-d it is seen that the initial cap is bounded by a highly irregular surface. Similar patterns are observed on the surface of rising thermals [10], and they are indicative of the turbulent nature of the flow inside the initial cap.

The slender plume below the cap can be considered as a steady structure, since it remains largely unchanged once developed to a certain height (see fig. 2c-f). A key feature of the slender plume is the continuous acceleration of the rising fluid which is evident from the decrease in plume diameter with height. In all experiments we performed, this steady plume was observed to break through the initial cap at some well-defined moment which we refer to here as t^* (see fig. 2d). The plume height at this instant will be denoted as h^*. On top of the rising plume another cap is formed the length scale of which does not directly depend on the size of the area source (fig. 2e), and which resembles the cap of a starting plume originating from a point source [6, 11]. The remnants of the initial cap, left behind by the plume's advancing front, are further diluted by the entrainment of ambient fluid and rise only slowly (fig. 2f) due both to the flow induced by the steady plume and to the residual buoyancy.

5. – Measurement results

The height h of the plume as a function of time t is depicted in fig. 4 for two series of experiments conducted with different buoyancy parameters F. The time t^* and the corresponding plume height h^* are marked with circles. Figure 4 shows that, as one may expect, in the dimensionless domain the plume rises faster for higher values of F. While all seven experiments for a buoyancy parameter of $F = 0.0672$ were performed with the identical set-up, the experiments for $F = 0.0348$ were conducted with different

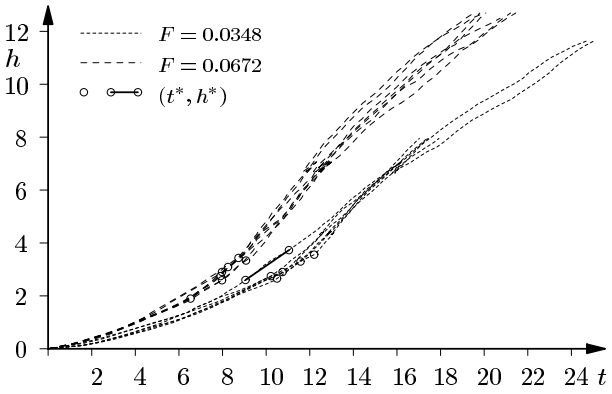

Fig. 4. – Dimensionless height h of the plume as a function of dimensionless time t for two series of experiments at different buoyancy parameters F. Circles indicate the instant when the plume breaks through the initial cap. Two circles connected with a line indicate that the time t^* could only be determined to be within the corresponding range.

values of $\tilde{r}_0$, $\tilde{g}'_0$ and $\tilde{Q}$ resulting in different ratios of tank width to source width and different dimensionless viscosities ν ranging between $1.69 \cdot 10^{-4}$ and $3.4 \cdot 10^{-4}$. This was done in order to examine whether or not viscous effects or the finite width (and height) of the tank have a substantial effect on the gross characteristics of the flow. The fact that the curves virtually collapse suggests that F is the only significant parameter.

From fig. 4 it is seen that t^*, *i.e.* the time the plume breaks through the initial cap, separates two different flow regimes: For times $t < t^*$ the plume accelerates, while for $t > t^*$ the upward motion of the plume slows down. In the subsequent section we will discuss separate integral models for these two flow regimes. The model for $t > t^*$ will require the instant of breakthrough as an input from the experiments, since a theory which allows us to predict t^* and h^* is not yet available. Research in that direction is currently under way. For the time being, we employ simple curve fits to obtain the functional dependence of these two quantities on F. From figs. 5 and 6 it is seen that

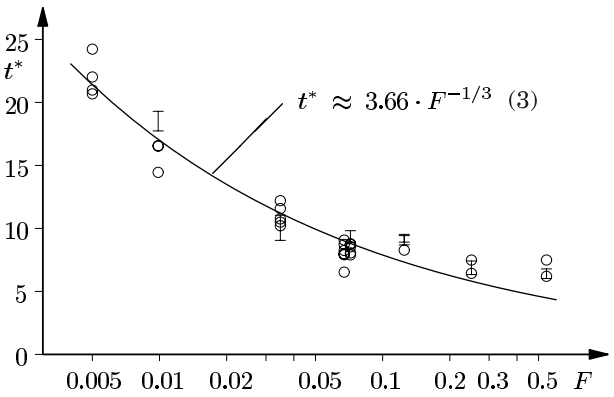

Fig. 5. – Time t^* when the plume breaks through the initial cap as a function of F. Bars indicate the time span in cases where t^* was not well defined. The solid line gives a least-squares fit to the experimental data.

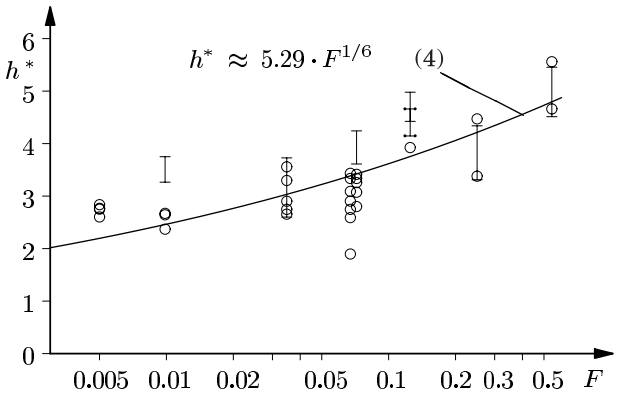

Fig. 6. – Height h^* of the plume at time t^* as a function of F. Bars indicate the time span in cases where t^* was not well defined. The solid line gives a least-squares fit to the data.

the approximations

$$t^* \approx 3.66 \cdot F^{-1/3}, \tag{3}$$

$$h^* \approx 5.29 \cdot F^{1/6} \tag{4}$$

appear to follow the experimental results quite well.

6. – Integral modeling

To describe the plume rise in the initial accelerating phase, *i.e.* before $t = t^*$, we will employ a theoretical model which is similar to the one put forth by Turner [6] for starting plumes above point sources. However, the plume above an area source differs from plumes over point sources in that the area source imposes an additional length scale on the flow that may be dominant in the early flow development. Plumes over area sources therefore do not develop in a self-similar fashion which is well illustrated in fig. 2. The assumption of self-similarity plays a key role in classical theory of starting plumes [6], but cannot be applied in our case. For brevity we will restrict the present discussion of our model to its essential features, but the reader is referred to [8] for a more detailed description.

To simplify the problem at hand we consider the shape of the initial cap to be a flattened sphere having a volume of $4/3\pi b_c^2 r_c$ inside which the buoyancy and the vertical velocity are constant. For this flattened sphere the balances of total mass, mass of buoyant material and momentum integrated over the volume of the cap lead to the following system of differential equations (for definition of the variables see fig. 1b):

$$\frac{4}{3}\frac{\mathrm{d}}{\mathrm{d}t}(b_c^2 r_c) = b_i^2 v_i - b_i^2 \frac{\mathrm{d}h_c}{\mathrm{d}t} + 2\alpha_c b_c^2 \frac{\mathrm{d}h_c}{\mathrm{d}t}, \tag{5}$$

$$\frac{4}{3}\frac{\mathrm{d}}{\mathrm{d}t}(b_c^2 r_c g_c') = b_i^2 v_i g_i' - b_i^2 g_i' \frac{\mathrm{d}h_i}{\mathrm{d}t}, \tag{6}$$

$$\frac{4}{3}\frac{\mathrm{d}}{\mathrm{d}t}\left(\frac{\mathrm{d}h_c}{\mathrm{d}t}(b_c^2 r_c + \kappa b_c^3)\right) = \frac{4}{3} b_c^2 r_c g_c' + b_i^2 v_i^2 - b_i^2 v_i \frac{\mathrm{d}h_i}{\mathrm{d}t}. \tag{7}$$

The rate of lateral spread of the initial cap, which gives the width of the cap b_c as a function of height h, we found to be fairly constant and determined it directly from our experiments. In eq. (5) the entrainment of ambient fluid into the cap is modeled by the usual entrainment hypothesis (see, *e.g.*, [12]) letting the amount of fluid entrained be proportional to the cap velocity and surface. For simplicity the latter is approximated by $2\pi b_c^2$. The constant of proportionality, the entrainment coefficient, is termed α_c in eq. (5). From the experiments we found α_c to be about 0.23, a value that agrees well with the entrainment coefficient of $\alpha_c = 0.25$ reported in the literature for the related problem of rising thermals [7]. Another simplification introduced is the assumption that the only drag exerted on the cap is due to ambient fluid accelerated from rest [7]. This effect is modeled with the added mass. In potential flows, the added mass of a flattened sphere is equal to the added mass of a sphere [13]. Therefore in eq. (7) we let the added mass be proportional to $4/3\pi b_c^3$ by a factor κ. From our experiments we determined κ to be about 1.2 which compares satisfactorily with the theoretical result of $\kappa = 11/16$ for a sphere touching a wall [13].

Different from rising thermals the initial cap is continuously fed with buoyant fluid by the plume underneath. In (5)-(7) all quantities indicated with an i denote conditions at the interface between the rising cap and the plume, and they need to be specified in order to close the system. From the experiments we observed that the flow within the accelerating plume is essentially laminar which allows to employ the analytic solution of a steady laminar plume with no entrainment $\alpha = 0$ given in [14]. This provides a simple relation between the interface conditions and the actual height h_i of the interface.

The system (5)-(7) was solved for h_c, r_c, and g_c' with a forth-order Runge-Kutta method, where the rise velocity at $t = 0$ was taken from the experimental observations as initial condition. The height h as a function of time t is shown in fig. 7, and a good agreement between numerical solutions and experimental data can be seen over the whole range of buoyancy parameters examined. Moreover, it is seen that the experimental results start to deviate from the theoretical curves from time t^* on. It should be emphasized that the present simplified model is not capable of predicting the time of transition t^*, since the breakthrough of the plume originates in inhomogeneities in the buoyancy distribution within the cap which are not taken into

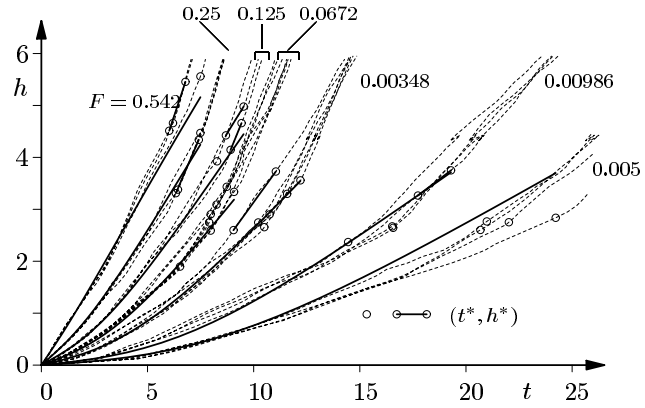

Fig. 7. – Experimental (dashed lines) and theoretical results for the rise of the initial cap (theoretical curves obtained from numerical solutions). Circles indicate t^*; two circles connected with a line indicate that t^* could only be determined to be within the corresponding range.

account. Clearly, to capture the breakthrough a much more refined approach would be required, and we have therefore employed the empirical relations for t^*, h^* given by (3), (4) in this first stage of our investigation.

For larger heights above the area source and $t > t^*$, one may expect that the flow approaches asymptotically a starting plume originating from a point source. For the latter the height h of the plume as a function of time t can be derived from relations given in [6] which yield

$$h = 1.01\alpha^{-1/2}F^{1/4}(t-t_0)^{3/4}, \tag{8}$$

where we have introduced a starting time t_0 at which the point source is turned on. In eq. (8) F and α are the buoyancy parameter and the entrainment coefficient of a fully turbulent steady plume, respectively. The factor 1.01 is obtained from constants which were determined empirically in [6].

From a visual examination of our experiments at later times we found that the developed plume has a virtual origin which is located close to the area source. We will therefore compare our measurements with results for related plumes which have the same buoyancy parameters F, but originate from point sources at $z = 0$. The two different types of plumes are sketched in fig. 8, where the initial cap of the plume above the area source has been drawn at its position at time t^*. To be able to directly compare the two plumes, we still need to determine the starting time t_0, *i.e.* the time delay with which the point source must be turned on, in order to make sure that both plumes reach the "critical" height h^* at the same time. It should be noted that t_0 will generally be different from zero (in fact larger than zero), since it is closely related to the amount of buoyancy contained in the initial cap which is left behind. The time t^* it takes the plume from an area source to reach the height h^* was already shown in fig. 5 and may well be approximated by (3). The time for Turner's starting plume to rise up to $z = h^*$ can be obtained from (8). The difference between the two rise times is equal to

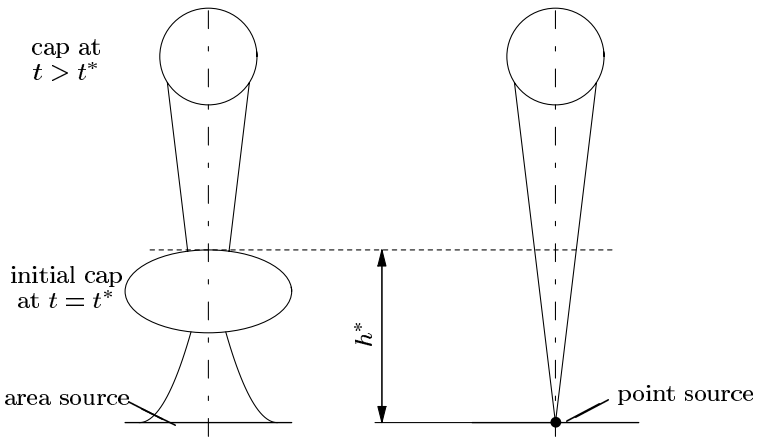

Fig. 8. – Sketch of a starting plume from an area source (left) and Turner's [6] starting plume originating from a point source (right).

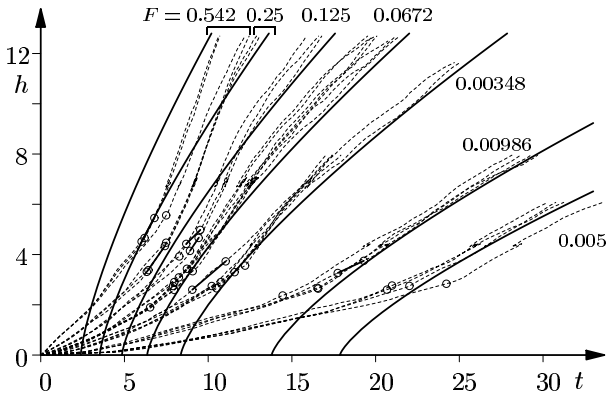

Fig. 9. – Experimental (dashed lines) and theoretical results for the height h of the plume as a function of time t; theoretical curves from eqs. (8), (9). Circles indicate t^*; two circles connected with a line indicate that t^* could only be determined to be within the corresponding range in the experiments.

the time delay t_0 for which one finds

$$t_0 = 3.66 F^{-1/3} - 9.10 \alpha^{2/3} F^{-1/9}. \tag{9}$$

The height of Turner's plume using (8), (9) is compared with our experimental data in fig. 9 where we have set the entrainment coefficient α to the standard value for plumes, *i.e.* $\alpha = 0.1$ [7]. The figure shows excellent agreement between theory and experimental data for t larger than t^*, in particular when F is small. Only for very large values of F the asymptotic solution appears to be approached more slowly, and is only reached for heights somewhat larger than h^*. For the largest buoyancy parameter examined, *i.e.* for $F = 0.542$, the tank is seen to be not deep enough for the asymptotic solution to develop fully. The experimental results suggest that in this case distances from the area source of some 20 times the source radius may be necessary, before the plume starts to follow the theoretical curve.

7. – Concluding remarks

Starting plumes above area sources were examined using a cubic tank filled with salt water into which dyed fresh water was released through a circular area source. The flow evolution was monitored with the aid of two videocameras, and from the recordings global quantities of the flow, such as height and width of the plume, were registered as a function of time. The gross behavior of the flow was found to depend primarily on a buoyancy parameter which is given by the ratio of inflow velocity to buoyancy velocity.

We have shown that starting plumes over area sources pass through two distinct regimes: The initial, transient phase consists in the formation of an intense buoyant vortex ring the strength and diameter of which directly depend on the conditions at the area source. The transition to the second flow regime occurs at some usually well-defined instant in time when the plume in the wake of the rising vortex ring has gained sufficient momentum to break through the ring. In the further flow

development the plume at larger heights may well be described by the classical theory for starting plumes above point sources. To predict the rise of both the initial vortex ring and the developed plume in the second flow phase, we have developed integral models which were briefly discussed. It was demonstrated that the model predictions are in good agreement with the experimental data.

REFERENCES

[1] DAVIES G. F., *Earth Planet. Sci. Lett.*, **99** (1990) 94.
[2] SPEER K. G., *Science*, **280** (1998) 1034.
[3] FANNELØP T. K., *Fluid Mechanics for Industrial Safety and Environmental Protection* (Elsevier Science B.V.) 1994.
[4] BETTELINI M. S. G. and FANNELØP T. K., *Appl. Ocean Res.*, **15** (1993) 195.
[5] MORTON B. R., TAYLOR G. I. and TURNER J. S., *Proc. R. Soc. London, Ser. A*, **234** (1956) 1.
[6] TURNER J. S., *J. Fluid Mech.*, **13** (1962) 356.
[7] TURNER J. S., *Buoyancy Effects in Fluids* (Cambridge University Press) 1979.
[8] FRIEDL M. J. *Bubble plumes and their interactions with the water surface*, Dissertation No. 12667 (Swiss Federal Institute of Technology (ETH)) 1998.
[9] SPARROW E. M., HUSAR R. B. and GOLDSTEIN R. J., *J. Fluid Mech.*, **41** (1969) 793.
[10] WOODWARD B., *Q. J. R. Meteor. Soc.*, **85** (1959) 144.
[11] TSANG G., *Atmos. Environ.*, **4** (1970) 519.
[12] TAYLOR G. I., *Dynamics of a mass of hot gas rising in air*, USAEC Report MDDC-919 LADC-276 (Los Alamos Scientific Laboratory) 1945.
[13] MILNE-THOMSON L. M., *Theoretical Hydrodynamics* (Macmillan & Co. Ltd., London) 1968.
[14] SCORER R. S., *Environmental Aerodynamics* (Ellis Horwood Ltd., Chichester) 1978.